Transactions, SMiRT-24
BEXCO, Busan, Korea - August 20-25, 2017
Division II

J-integral analysis of a sub-clad crack under PTS transient

Wenlong Luo[1], Meiyan Li[2], Yuebing Li[3], Zengliang Gao[4],
[1] Postgraduate (student), ZheJiang University of Technology, China
[2] Postgraduate (student), ZheJiang University of Technology, China
[3] PhD, ZheJiang University of Technology, China
[4] Professor, ZheJiang University of Technology, China

ABSTRACT

The inner surface of the reactor pressure vessel is often clad with stainless steel. Near the interface between the base material and cladding metal, it is easy to produce some embedded cracks during the welding process. A sub-clad crack near the interface may be characterized as a semi elliptical crack or an elliptical crack. It is necessary to check which characterization mSethod is conservative and suitable for engineering application.

In this work, a subsurface crack near the surface is characterized to be 3 different models, including surface crack, subclad semi-elliptical crack, and embed elliptical crack. The fracture mechanics parameters are calculated by finite element method for the 3 models with same depth under a typical pressurized thermal shock transient. The J-integrals are compared to check which model is more reasonable. The results show that J-integral at the deepest point for surface crack model is greater than the subsurface crack models. At the same time, the SIF transferred from J-integral at the deepest point for surface crack model is about twice of the subsurface cracks. From the point of view of the work in FE model and calculation, a subclad model for the flaw can be used to evaluate the structure integrity of RPV under PTS.

KEY WORDS: sub-clad crack, pressurized thermal shock, fracture mechanics

INTRODUTION

As an important component in nuclear power plant, the reactor pressure vessel (RPV) is cladded with stainless steel to prevent corrosion and radiation embrittlement(Choi et al., 2000). The structural integrity assessment of RPV with possible micro-cracks is a complex task, since the welding and heat treatment processes and the mismatch in the thermo-mechanical properties of the two bonded materials in general result in complex residual and thermally induced stress fields, which is caused from some pressurized thermal shock (PTS) transients (Ferreñoa et al., 2010). These micro cracks may grow due to the service loading conditions. When a crack is found during the in-service inspection, the structural intensity of RPV should be evaluated according to the fracture mechanics analysis procedure, such ASME Sec. XI, RSE-M, KTA rules, etc.

However, flaws may exist at the interface between the base metal and the clad metal. If such flaws are detected, they shall be sized by the bounding rectangle or square for the purpose of description and dimensioning. The dimensions of a flaw shall be determined by the size of a rectangle or square that fully contains the area of the flaw. Then the flaw is idealized into either semi-elliptical surface crack or elliptical subsurface crack. The cracks near the interface can be characterized to be either a semi-elliptical sub-clad crack which is contained by the clad metal, or an elliptical subsurface crack which lies exclusively in the base metal. Therefore, it is important to investigate the fracture behavior of these subsurface cracks, which is valuable for cladded components with subsurface cracks near the interface(Blauel et al., 1997; Mukhopadhyay et al., 1998).

FLAW CHARACTERIZATION

It is assumed that a subsurface crack is detected near the interface, as shown in Figure 1. The crack is sized by the rectangle with $l \times 2d$. With the consideration of surface interaction, a subsurface indication shall be considered a surface flaw if the distance S from the flaw to the nearest surface of the component is less than $0.4d$. If the nearest surface of the component is clad, S shall be measured to the clad-base metal interface in accordance with ASME Sec. XI IWA-3300. The criteria have been checked by finite element analysis(Coules. H. E., 2016; Jörg Hohe et al., 2010; IAEA, 2010).

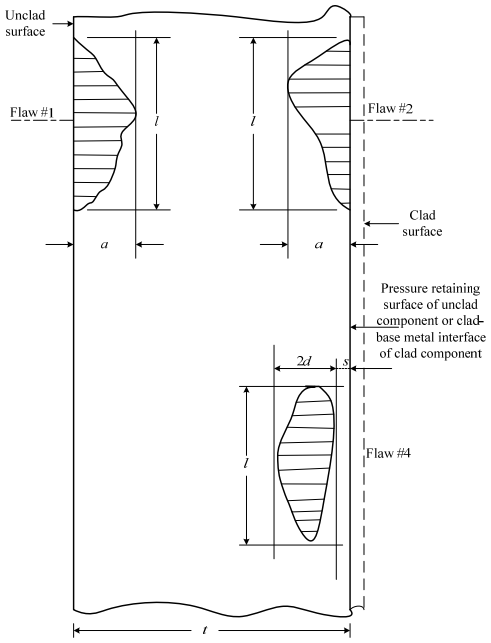

Figure 1 Planar flaws near the interface in clad components

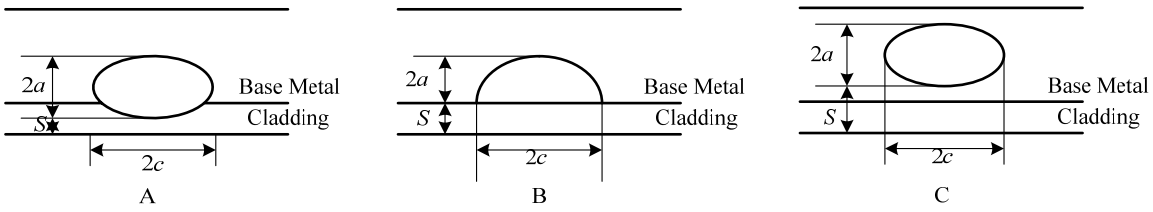

Figure 2 The subsurface crack in clad components

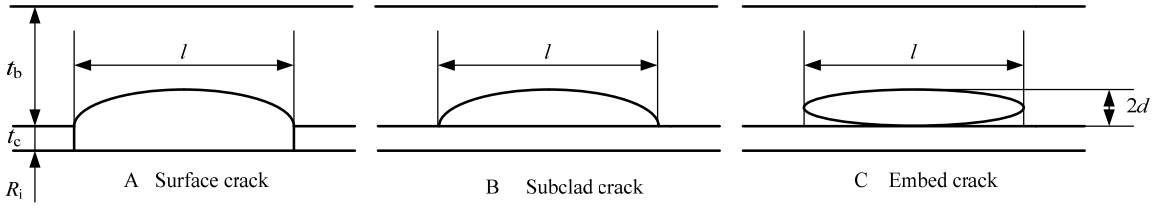

Figure 3 crack size and characterization in clad component

However, in IWB-3600 “analytical evaluation of planar flaws”, the flaws in clad components are classified into 5 categories including 2 categories of surface flaws and 3 categories of subsurface flaws, as

shown in Figure 2. Category A shows the subsurface crack which lies in both the clad and the base material. Category B represents the subsurface crack which is contained by the clad material and is classified as sub-clad crack. Category C is the subsurface crack which lies exclusively in the base material. All three categories should be treated as either a surface or a subsurface crack depending on the relation between S and d as shown in Figure 2. It can be seen that the distance S from the flaw to the nearest surface of the clad component is measured to the vessel internal surface, which is disaccord with IWA-3300.

In the work, it is assumed that a subsurface crack is detected near the interface, with l=60mm, and $2d$=10mm, as shown in Figure 3. The distance S from the flaw to the nearest surface of the clad component is 12mm, which is measured to the vessel internal surface. Three categories are characterized, including surface semi-elliptical crack, sub-clad semi-elliptical crack, and embed elliptical crack.

MATERIAL AND LOAD CONDITIONS

The base material of the RPV is made of ferrite low alloy steel and the cladding is made of austenitic stainless steel. Only the beltline region of the vessel is considered in this work. The thermo-mechanical properties of the base metal and cladding metal at different are listed in Table 1, which are adopted from the IAEA CRP-9 PWR benchmark (IAEA, 2010).

Table 1 Material Properties

	Base Metal		Cladding	
Temperature T [°C]	20	300	20	300
Expansion α [10^{-6} °C^{-1}]	10.9	12.9	16.4	17.7
Conductivity λ [W/(m·°C)]	54.6	45.8	14.7	18.6
Specific Heat c [J/(kg·°C)]	488.7	568.5	471.8	569.2
Density ρ [kg/mm^3]	7.6	7.6	7.6	7.6
Yield Strength σ_y [Mpa]	588	517	380	270
Young's Modulus E [Mpa]	204000	185000	197000	176500
Possion Ratio υ	0.3	0.3	0.3	0.3

Table 2 IAEA CRP 9 PWR PTS benchmark

Time [s]	Pressure [Mpa]	Fluid temperature [°C]	Heat Exchange coefficient [W/(m^2·°C)]
0	15.3	295	24125
45	7.8	287	24696
165	7.0	276	3453
255	7.3	279	1054
300	5.7	268	6232
375	5.5	261	1757
615	5.1	251	4834
1515	4.0	206	1581
2865	2.9	152	1838
4695	2.0	59	1147
6015	1.5	37	992
7125	2.5	48	877
7185	16.8	49	790
8970	17.1	69	602
13290	17.0	96	710
14025	17.1	106	1229
14985	17.1	115	1057

Meanwhile, the load condition is also adopted from the benchmark. A potential scenario for a

pressurized water reactor is that its RPV has to withstand some pressurized thermal shock (PTS) transients, which are characterized by severe cooling of the core together with or followed by repressurization. A typical PTS with repressurization is considered as shown in Table 2.

FINITE ELEMENT MODELLING

Finite element analysis (FEA) is conducted for the fracture mechanics behavior of the cracks. Elastic-plastic FEA is carried out using the general finite element program ABAQUS. Because of the symmetric structure and load condition, only one quarter of the vessel beltline is modeled. Figure 4 shows a typical mesh model with 8-node hexahedron element. The stress field around the crack is characterized by a stress singularity at the crack tip. The crack tip is modeled with a focused wedge-type elemen t (Pachoud et al , 2017). J-integral is computed based on the domain integral.

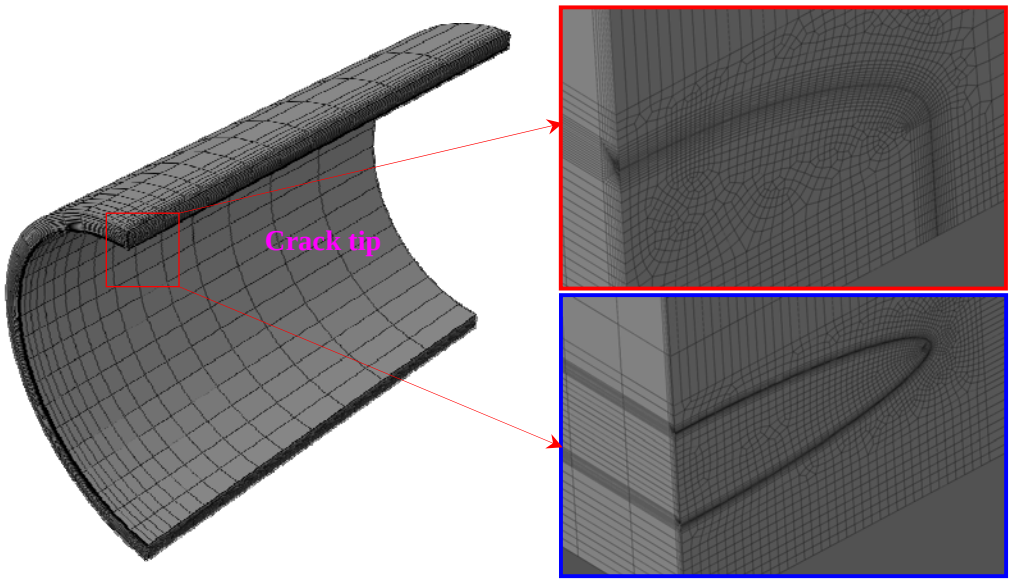

Figure 4 Finite Element Mesh

ANALYSIS RESULTS

J-integrals at the deepest point of crack are showed in Figure 5. As we can be seen, the J-integrals for different cracks almost have a similar tendency. Under the PTS transient, J-integrals decline rapidly in the initial stage due to the release of internal pressure. With the temperature drop, the thermal stress increases, which results in the raise of J-integrals. When repressurization starts up, J-integral reaches a maximum. It also can be seen that J-integral of surface crack is much larger than another two models.

The J-integrals along the crack tip are shown in Figure 6 for 3 crack models. For surface crack, nodes located in the cladding have much larger J-integrals than the nodes in base metal, which can be 79.4% higher than the deepest node in base metal. For subclad semi-elliptical crack, J-integrals decreased as the point of calculation moves along the crack tip line from the deepest point to the surface point. For subsurface elliptical crack, J-integrals scattered in symmetric distribution about the elliptical axis.

For the investigation of the fracture behavior, J-integral is transferred to stress intensity factor(SIF) assuming plane strain condition, with the lack of data in J-integral of material(Samal, M. K., 2013).

$$K = \sqrt{\frac{EJ}{1-\nu^2}} \tag{1}$$

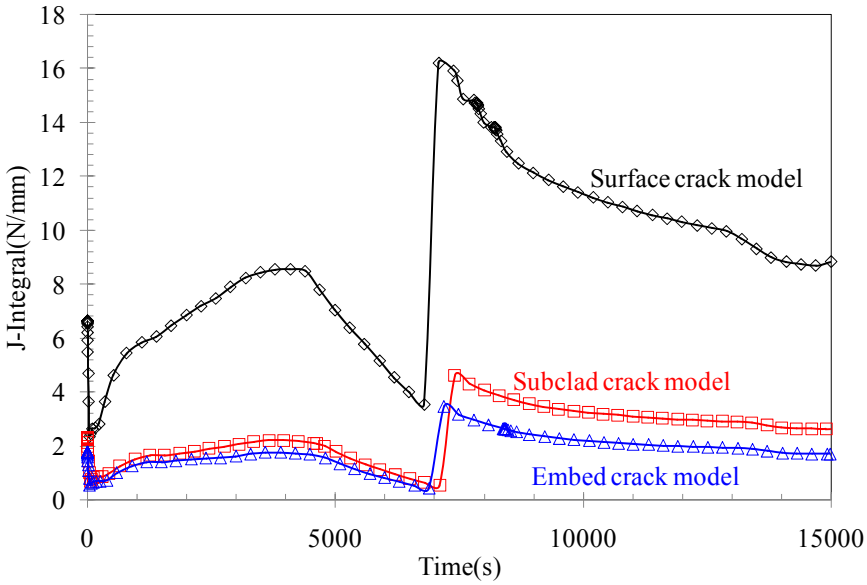

Figure 5 The maximum J-integral for different crack models

The maximum values at the deepest point and surface point during the whole transient for the 3 models are listed in Table 3. The SIF at the deepest point for surface crack model is about twice of the subsurface cracks(including subclad and embed crack model). This is reasonable since that the surface crack has a larger crack depth with crack depth plus the thickness of cladding ($2d+t_c$) , as shown in Figure 3. For the subsurface crack model, SIFs for subclad crack model are very close to embed crack model. However, the subclad model may be more suitable from the point of view of the work in FE model and calculation. If the flaw is characterized to be a surface crack, it will cause a overly conservative result. Therefore, a subcrack model for the flaw can be used to evaluate the structure integrity of RPV under PTS.

Table 3 Comparison of stress intensity factors for different models (MPa·m$^{1/2}$)

	Surface crack	Subclad semi-elliptical crack	Embed elliptical crack
Deepest point	73.18	31.96	27.73
Surface point	59.86	13.75	10.11

CONCLUSION

The objective of the present study was to investigate the effect of idealized models for a real defect. Total of 3 three-dimensional finite element analyses were performed to calculate the J-integral for surface crack model, subclad semi-elliptical crack model, and embed elliptical crack model with same depth under a typical PTS transient.

For surface crack, nodes located in the cladding have much larger J-integrals than the nodes in the base metal. For the crack tip in the base metal, J-integral at the deepest point for surface crack model is greater than the subsurface crack models. At the same time, the SIF transferred from J-integral at the deepest point for surface crack model is about twice of the subsurface cracks. If the flaw is characterized to be a surface crack, it will cause a overly conservative result. For the two subsurface crack models, the J-integrals are very close to each other. From the point of view of the work in FE model and calculation, a subclad model for the flaw can be used to evaluate the structure integrity of RPV under PTS.

In the next work, it is necessary to determine how to characterize a real defect near the cladding and get a more reasonable and economical result for the structure integrity of RPV under PTS.

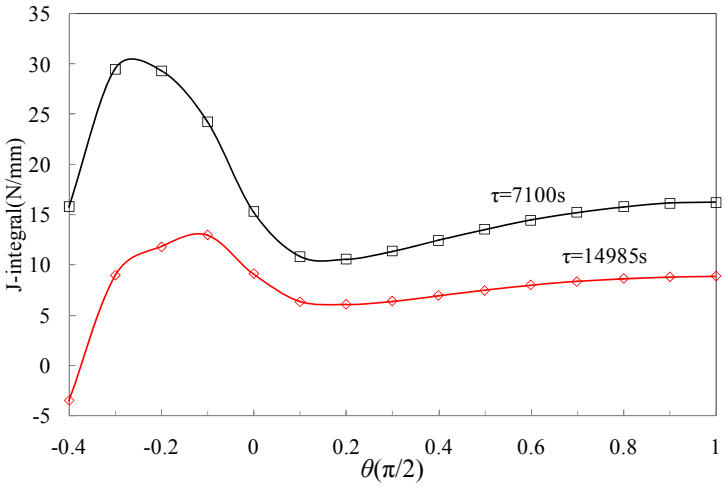

a) Surface semi-elliptical crack

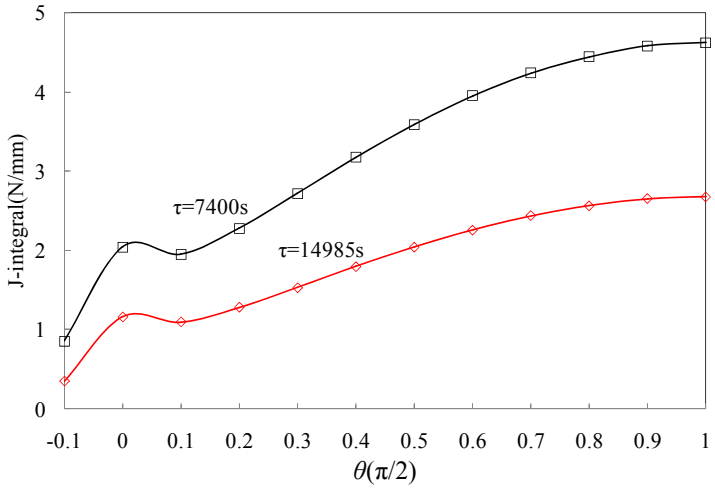

b) Surclad semi-elliptical crack

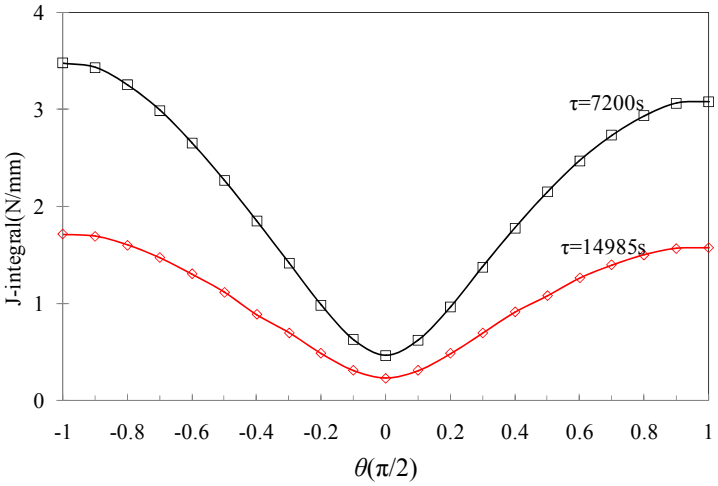

c) Subsurface elliptical crack

Figure 6 The variation of J integral along the crack tip

REFERENCES

Blauel, J. G., Hodulak, L., Nagel, G., Schmitt, W., Siegele. D. (1997). "Effect of cladding on the initiation behaviour of finite length cracks in an RPV under thermal shock," *Nuclear Engineering and Design,* 176 179-188.

Choi, S. N., Jang, K. S., Kim, J. S., Choi, J. B., and Kim, Y. J. (2000). "Effect of cladding on the stress intensity factors in the reactor pressure vessel," *Nuclear Engineering and Design*, 101-111.

Coules. H. E. (2016). "Stress intensity interaction between dissimilar semi-elliptical surface cracks," *International Journal of Pressure Vessels and Piping,* 146 55-64.

Ferreñoa, D., Lacallea, R., Gorrochateguib, I., Gutiérrez-Solanaa. F. (2010). "Analysis of dynamic conditions during thermal transient events for the structural assessment of a nuclear vessel," *Engineering Failure Analysis,* 17 894-905.

International Atomic Energy Agency, 2010. Pressurised thermal shock in nuclear power plants: good practices for assessment. In: IAEA-TECDOC-1627. IAEA, Austria.

Jörg Hohe, Marcus Brand, Dieter Siegele. (2010). "Behaviour of sub-clad and through-clad cracks under consideration of the residual stress field," *Engineering Fracture Mechanics,* 77 217-228.

Mukhopadhyay, N. K., Pavan Kumar, T. V., Chattopadhyay, J., Dutta, B. K., Kushwaha. H. S. (1998). "Deterministic assessment of reactor pressure vessel integrity under pressurised thermal shock," *International Journal of Pressure Vessels and Piping,* 75 1055-1064.

Pachoud, A. J., Manso, P. A., Schleiss, A. J. (2017). "Stress intensity factors for axial semi-elliptical surface cracks and embedded elliptical cracks at longitudinal butt welded joints of steel-lined pressure tunnels and shafts considering weld shape," *Engineering Fracture Mechanics*, 179 93-119.

Samal, M. K., Sanyal, G. (2013). "A Generalized Geometric Shape Function for Evaluation of SIF Values of Thin-Walled Axially-Cracked Fuel Pin Specimens," *Procedia Engineering*, 55 367-373.